In situ high-temperature nuclear magnetic resonance characterization of structural evolution in pure gallium melt

Liang Peng,[1,2] Enyi Chen,[1] Shiyu Liu,[1] Xun Liu,[1] and Yao Yu[1,2,*]

[1]*School of Materials Science and Engineering and State Key Laboratory of Materials Processing and Die and Mold Technology, Huazhong University of Science and Technology, Wuhan 430074, China*

[2]*Wuhan National High Magnetic Field Center, Huazhong University of Science and Technology, Wuhan 430074, China*

(Received 22 January 2019; revised manuscript received 3 June 2019; published 26 September 2019)

The structure of liquid gallium (Ga) is a long-standing issue in the studies of metallic liquids. In this paper we investigate pure Ga melt in the temperature range of 307–1356 K by high-temperature ^{69}Ga and ^{71}Ga NMR. A structural crossover at around 1000 K is revealed through the analyses of NMR observables including the Knight shift and the spin-lattice relaxation time, which may result from the temperature-induced structural evolution of the covalently bonded clusters in pure Ga melt. However, structure and diffusivity anomalies around 450 and 730 K at ambient pressure, which may be induced by the liquid-liquid critical point, are not observed.

DOI: 10.1103/PhysRevB.100.104113

I. INTRODUCTION

Ga is the most important constituent for Ga-based room-temperature liquid metal alloys, which have promising applications in heat transfer, wearable computing, stretchable electronics, and biomimetic mechanics [1–4]. Following the paradigm of the structure-property relationship in materials research, a good understanding of the liquid structure of Ga is of great importance to improve the application of the Ga-based liquid materials. So far, liquid Ga has already attracted extensive attention for the unusual dimer-constructed α-Ga crystal [5,6] and the negative melting slope. However, several problems related to liquid Ga structure are still unsolved. First, the high-q shoulder in the static structure factor $S(q)$ of liquid Ga is a long-standing problem. It is suggested that the shoulder peak could result from the short-range or medium-range Ga clusters [7–9]. Experimental and theoretical studies on individual Ga clusters have shown that some clusters can persist to temperatures far above the melting point of α-Ga [10–16]. However, whether the case of clusters is the true case in bulk liquid Ga is still unknown. Second, structure evolution of liquid Ga has also attracted much attention [17,18]. Recently, a structure change in pure Ga melt at about 1000 K was reported [19], while the nature of the structure change is still to be explored. Third, the liquid-liquid critical point (LLCP) hypothesis [20–22], which developed to explain the anomalies in water, is also suggested to be applicable to liquid Ga. Theoretical calculation predicts that the liquid-liquid transition and LLCP are located at negative pressure [23], and recent researches suggest that the LLCP in Ga may induce density anomaly, structure anomaly, and diffusivity anomaly which can extend to high temperature at ambient pressure [24]. It is important to search for signatures of the predicted anomalies. Thus, a careful high-temperature experimental examination with a powerful method is needed to elucidate these problems related to the liquid Ga structure.

NMR is a versatile method in studying the metallic liquids [25–27]. Unlike diffraction methods (i.e., neutron and x-ray diffraction, which are based on pairwise distribution), the NMR observables, including the Knight shift and relaxation times, can provide information about the overall local structure and dynamic changes of metallic liquids. Pure Ga melt at temperatures near the melting point has been carefully examined by NMR methods [28–31]. While at temperatures well above the melting point, the information revealed by previous NMR studies is ambiguous due to the limited experimental accuracy and data points [32].

In this paper, we study pure Ga melt in the temperature range of 307–1356 K by high-temperature ^{69}Ga and ^{71}Ga NMR. Below and above 1000 K different temperature dependencies of Knight shift and spin-lattice relaxation time have been observed. Further analyses imply that complex clusters exist in pure Ga melt and the changes of the NMR observables may result from the temperature-induced structural evolution of the covalently bonded Ga clusters. A continuous variation of the electronic structure is shown and no hysteresis is observed between the heating and cooling curves, suggesting that the structure change at around 1000 K is a crossover which may be due to the weak cooperativity induced by the low constraint of the covalent bonds. Moreover, the predicted structure and diffusivity anomalies as a consequence of the critical fluctuation approaching LLCP are not observed at ambient pressure.

II. EXPERIMENTAL METHOD AND RESULTS

High-purity Ga (99.999%, Sinopharm Chemical Reagent Co., Ltd.) was used in our experiments. The samples were prepared by vacuum sealing the pure Ga particle (about 80 mg) in the quartz tube at room temperature. *In situ* high-temperature NMR experiments were carried out in a magnetic field of 9.4 T (Bruker Ascend 400WB) using a home-made high-temperature NMR probe. A standard 90-deg one-pulse sequence was used with pulse widths of 9 and 7 μs for ^{69}Ga

*ensiyu@mail.hust.edu.cn

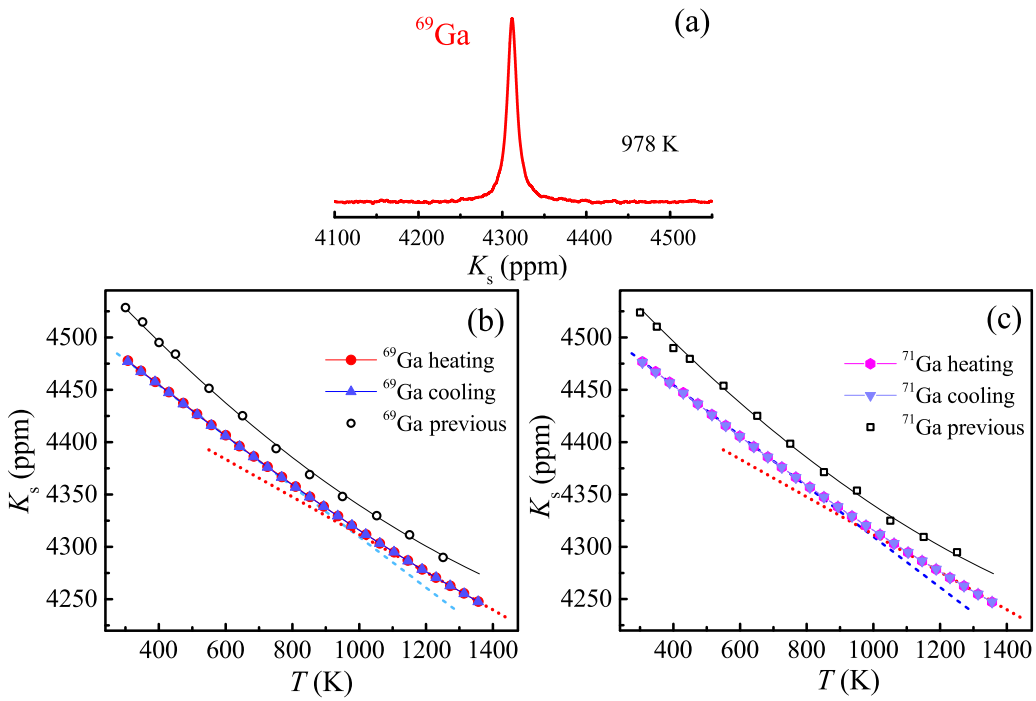

FIG. 1. (a) A ^{69}Ga NMR spectrum acquired at 978 K during consecutive heating. (b, c) Temperature (T) dependences of the Knight shift (K_s) of ^{69}Ga and ^{71}Ga, respectively. The light blue dashed line in (b) and the blue dashed line in (c) represent the fitting curve with a slope of $-0.24\,\mathrm{ppm\,K^{-1}}$, and the red dotted lines in both (b) and (c) represent the fitting curve with a slope of $-0.19\,\mathrm{ppm\,K^{-1}}$. The open black circles in (b) and the open black squares in (c) represent the K_s of ^{69}Ga and ^{71}Ga reported previously by Kerlin and Clark [32], and the black solid curves in both (b) and (c) represent the quadratic fitting curve in their paper.

and ^{71}Ga, respectively. Recycle delay time was 10 ms in all measurements. A total of 4096 scans were accumulated for each measurement to get a good signal-to-noise ratio. A series of ^{69}Ga and ^{71}Ga spectra were taken with consecutively increasing temperatures from 307 to 1356 K. At each temperature the system was equilibrated for 5 min before measurement. After completing the heating experiments at 1356 K, the sample was kept for 1 h before the cooling experiments. Again, a series of ^{69}Ga and ^{71}Ga spectra were taken with consecutively decreasing temperatures down to 307 K. All ^{69}Ga and ^{71}Ga NMR spectra were referenced to $1\,\mathrm{M\,Ga(NO_3)_3}$ aqueous solution. The temperature was carefully calibrated by using the melting point of pure indium, aluminum, and copper, with the temperature accuracy of ± 2 K. Three samples were tested in three independent stepwise heating and cooling experiments to ensure accuracy.

In the whole tested temperature range, all of the ^{69}Ga and ^{71}Ga spectra show a single narrow peak of Lorentzian shape, which suggests that the Ga melt is in a single macroscopic phase. Figure 1(a) shows the NMR spectrum of ^{69}Ga acquired at 978 K during the consecutive heating process as an example. The peak position of the spectrum represents the Knight shift (K_s) which is sensitive to the structure change, and the full width at half maximum (FWHM) of the peak ($\Delta\nu$) can provide structural and dynamic information of the pure Ga melt. The temperature (T) dependences of K_s of ^{69}Ga and ^{71}Ga measured during our isothermal heating and cooling experiments are shown in Figs. 1(b) and 1(c). They are identical and overlap with each other. The heating curve of the K_s varies linearly with a slope of $-0.24\,\mathrm{ppm\,K^{-1}}$ below 800 K, but starts deviating from the linear variation at about 800 K, and varies linearly again but with a different slope of $-0.19\,\mathrm{ppm\,K^{-1}}$ above 1100 K. The extrapolations of the linear fittings of the temperature dependences of K_s below 800 K and above 1100 K intersect at about 1000 K. The cooling curve of the K_s reproduces the heating curve perfectly in the whole temperature range, and no hysteresis is observed. The previously reported [32] K_s values of ^{69}Ga and ^{71}Ga are also shown in Figs. 1(b) and 1(c). Similar tendencies of K_s between our measured data and previously reported data can be observed and a tendency change around 1000 K seems also plausible in the previously reported data. However, with limited data points and relatively large error, a common quadratic variation of K_s in the whole tested temperature region was postulated in the previous paper. The absolute value difference of K_s between our data and previous reported data may be caused by different calibration methods.

Spin-lattice relaxation is an important process in NMR experiments which can provide deeper insight into the structure and dynamic changes [25,26]. As the extreme narrowing limit is usually assumed in pure Ga melt [31,33], the spin-lattice relaxation time (T_1) is equal to the spin-spin relaxation time (T_2), which can be calculated from $\Delta\nu$ by [26,34]

$$T_2 = (\pi\,\Delta\nu)^{-1}. \tag{1}$$

The T dependences of $(T_1T)^{-1}$ of ^{69}Ga and ^{71}Ga using T_1 calculated from our experimentally measured FWHM are

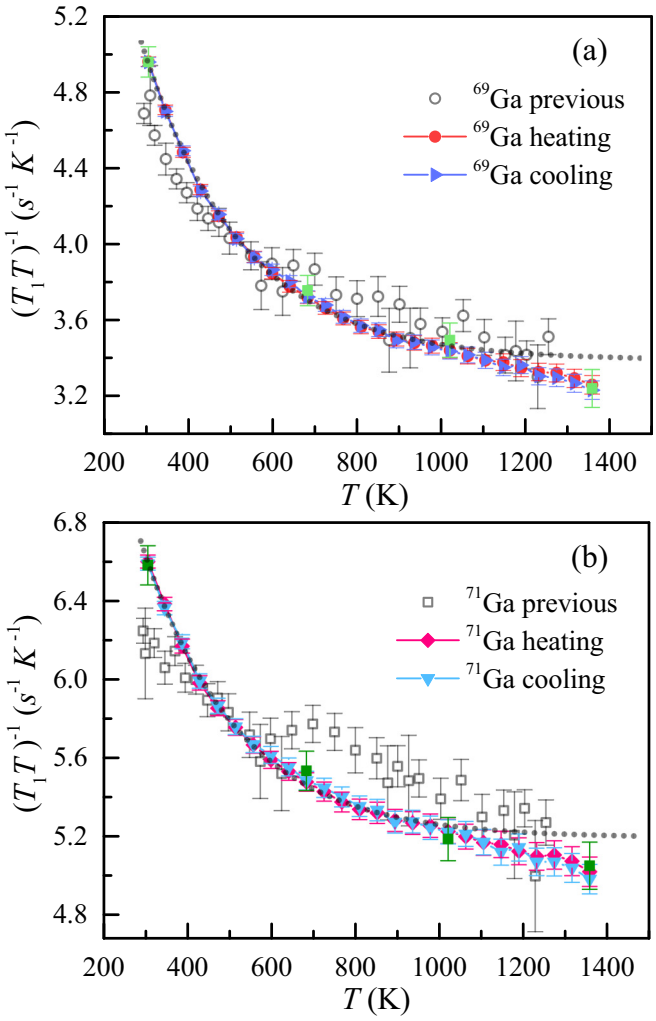

FIG. 2. T dependences of $(T_1T)^{-1}$ of ^{69}Ga and ^{71}Ga. The open black circles in (a) and the open black squares in (b) represent the $(T_1T)^{-1}$ of ^{69}Ga and ^{71}Ga reported previously [32]. The solid green squares in (a) and solid dark green squares in (b) are calculated using our measured T_1 by inverse-recovery method at 307, 683, 1019, and 1356 K to verify the equality of T_1 and T_2. Dotted lines are guides for the eye.

plotted in Fig. 2. The heating curve of $(T_1T)^{-1}$ of ^{69}Ga decreases with T increasing in the whole tested temperature region as shown in Fig. 2(a), and different T dependences can be observed below and above 1000 K. The heating curve of $(T_1T)^{-1}$ of ^{71}Ga exhibits the same trends as that of ^{69}Ga as shown in Fig. 2(b). The cooling curves of $(T_1T)^{-1}$ for both ^{69}Ga and ^{71}Ga of our measured data reproduce the heating curves within error, and no hysteresis is observed. Previously reported [32] $(T_1T)^{-1}$ values of ^{69}Ga and ^{71}Ga are also replotted in Fig. 2, which are comparable with our $(T_1T)^{-1}$ data. The measurement of the previously reported T_1 data may be limited to the measuring method and the setups. The inverse-recovery method [25] was applied in the previous measurement, while T_1 can be determined by both inverse-recovery method and calculating from the FWHM if T_1=T_2 is applicable. Determination of T_1 from the FWHM avoids some procedures that could introduce errors in the inverse-recovery method (e.g., measuring spectra at different

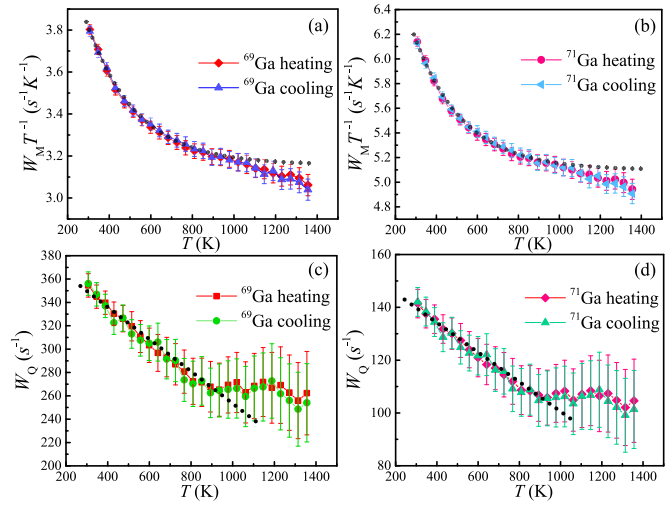

FIG. 3. T dependences of the magnetic relaxation rate divided by T (W_MT^{-1}) and T dependences of the quadrupole relaxation rate (W_Q) calculated using our T_1 data. (a, b) T dependences of W_MT^{-1} of ^{69}Ga and ^{71}Ga, respectively. (c, d) T dependences of W_Q of ^{69}Ga and ^{71}Ga, respectively. Dotted lines are guides for the eye.

inverse delay time and fitting), and it is also easier and more accurate to determine the T_1 from the FWHM with a more advanced superconducting magnet and NMR spectrometer.

As ^{69}Ga and ^{71}Ga nuclei possess electric quadrupole moments, two main processes may contribute to T_1 in pure Ga melt, the magnetic relaxation induced by the magnetic interaction and the quadrupole relaxation induced by the interaction of the electric-field gradient [27,35]. In our experiments, both ^{69}Ga and ^{71}Ga were measured, and the total relaxation rate (W) for each isotope of Ga can be written as [26]

$$W^{69} = 1/{T_1}^{69} = W_M^{69} + W_Q^{69}, \tag{2a}$$

$$W^{71} = 1/{T_1}^{71} = W_M^{71} + W_Q^{71}, \tag{2b}$$

where 69 and 71 denote the two isotopes of Ga, and W_M and W_Q are the magnetic relaxation rate and the quadrupole relaxation rate, respectively. Consequently, the contributions of the magnetic relaxation and the quadrupole relaxation for each isotope can be separated as [32,36]

$$W_M^{69} = (W^{69} - R_Q W^{71})/(1 - R_Q/R_M), \tag{3a}$$

$$W_M^{71} = W_M^{69}/R_M, \tag{3b}$$

$$W_Q^{69} = (W^{69} - R_M W^{71})/(1 - R_M/R_Q), \tag{3c}$$

$$W_Q^{71} = W_Q^{69}/R_Q, \tag{3d}$$

where

$$R_M = (\gamma_{69}/\gamma_{71})^2, \tag{4}$$

$$R_Q = [f(I_{69})/f(I_{71})](Q_{69}/Q_{71})^2, \tag{5}$$

$$f(I) = [(2I+3)/I^2(2I-1)], \tag{6}$$

γ is the nuclear gyromagnetic ratio, Q is the nuclear quadrupole moment, and I is the nuclear spin. Figure 3 shows the T dependences of W_MT^{-1} and W_Q for both isotopes of Ga

calculated from our T_1 data by Eqs. (2) and (3). The $W_M T^{-1}$ of ^{69}Ga decreases with increasing T during the whole tested temperature range as shown in Fig. 3(a). Different T dependences of $W_M T^{-1}$ below and above 1000 K are observed. Figure 3(b) shows the $W_M T^{-1}$ of ^{71}Ga, which has the same trends as that of ^{69}Ga. As discussed below, the change of the T dependence on the $W_M T^{-1}$ curves implies the structure change of Ga melt. Figure 3(c) shows the T dependence of W_Q of ^{69}Ga. Below and above 1000 K different T dependences of W_Q are observed, and at T above 1000 K W_Q decreases with a much slower rate than that at T below 1000 K. The T dependence of W_Q of ^{71}Ga also reveals the same tendency as that of ^{69}Ga as shown in Fig. 3(d). W_Q reflects the diffusional motion in metallic liquids [37–39]. The change of the T dependence of W_Q for both ^{69}Ga and ^{71}Ga at about 1000 K implies a kinetic change of the pure Ga melt. The cooling curves of $W_M T^{-1}$ and W_Q for both ^{69}Ga and ^{71}Ga reproduce the heating curve within error, and no hysteresis is observed.

III. DISCUSSION

With limited accuracy and data points, the structure and kinetic information at high temperature had not been analyzed systematically in previous NMR studies of pure Ga melt [28,32]. In our experiments, with improved accuracy (K_s error < 0.5 ppm) and more data points, a structure change was revealed by the slope change of K_s. Moreover, with more accurate relaxation results ($\Delta\nu$ error $< 1.5\%$), a deeper insight into the structure and kinetic changes can be obtained.

In pure Ga melt four mechanisms may contribute to K_s, which can be written as [27]

$$K_s = K_d + K_{CP}^s + K_{CP}^p + K_{orb}. \quad (7)$$

K_d comes from the direct hyperfine interaction of the s-state electrons, which can be further expressed as [40]

$$K_d = (8\pi/3)\chi_s \Omega \langle |u_F(0)|^2 \rangle, \quad (8)$$

where χ_s is the spin susceptibility per unit volume of s electrons, Ω is the atomic volume, and $\langle |u_F(0)|^2 \rangle$ is the averaged probability density at the nucleus of s-like Fermi-surface electrons; K_{CP}^s and K_{CP}^p are the s-core polarization and p-core polarization contribution, respectively; and K_{orb} is the orbital contribution. As the static interaction leads to the resonance frequency shift, the dynamic part of the contact hyperfine interaction is the chief mechanism of the magnetic relaxation [27]. For the situation with only K_d contributing to K_s, the magnetic relaxation rates W_M and K_d are related by the modified Korringa relation [41–43]

$$\frac{W_M}{T K_d^2} = \left(\frac{4\pi k_B}{\hbar}\right)\left(\frac{\gamma}{\gamma_e}\right)^2 K(\alpha)_d, \quad (9)$$

where γ_e is the electronic gyromagnetic ratio, k_B is Boltzmann's constant, $\hbar$ is the reduced Planck constant, and $K(\alpha)_d$, which is believed to be a constant, is the correction factor accounting for the effects of electron correlation and exchange on the Knight shift and relaxation rate. However, the different contributions to K_s cannot be separated experimentally. Simplify the expression of K_s as

$$K_s = K_d + K_{other}. \quad (10)$$

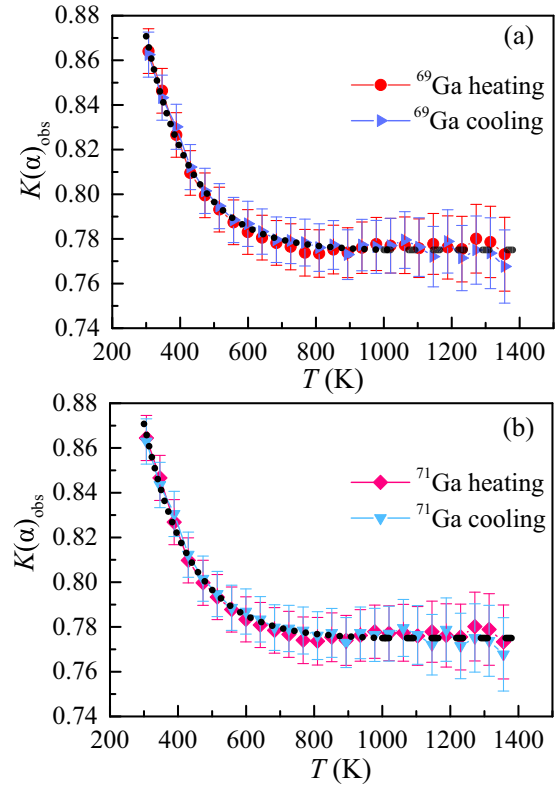

FIG. 4. T dependences of $K(\alpha)_{obs}$. (a) $K(\alpha)_{obs}$ of ^{69}Ga during consecutive heating (red circles) and cooling (blue triangles). (b) $K(\alpha)_{obs}$ of ^{71}Ga during consecutive heating (pink rhombi) and cooling (light blue triangles). The dotted lines and the dashed lines are guides for the eye.

The experimentally observed $K(\alpha)_{obs}$ fulfills the expression [32]

$$\frac{W_M}{T K_s^2} = \frac{W_M}{T(K_d + K_{other})^2} = \left(\frac{4\pi k_B}{\hbar}\right)\left(\frac{\gamma}{\gamma_e}\right)^2 K(\alpha)_{obs}. \quad (11)$$

Combine Eq. (11) with Eq. (9) to obtain

$$K(\alpha)_{obs} = \frac{K(\alpha)_d}{(1 + K_{other}/K_d)^2}. \quad (12)$$

Thus, the $K(\alpha)_{obs}$ characterizing the change of K_{other}/K_d is an indicator of the electronic structure change. Figure 4 plots the T-dependent $K(\alpha)_{obs}$ calculated from Eq. (11). For both isotopes of Ga, $K(\alpha)_{obs}$ vary the same, which shows a decrease with T increasing at T below 1000 K but remains invariant at T above 1000 K. These results indicate that K_{other}/K_d increases with T below 1000 K and K_{other}/K_d stays constant above 1000 K. The cooling curve of $K(\alpha)_{obs}$ reproduces the result of the heating curve in the whole tested temperature range, and no hysteresis is observed.

It is suggested that the bonding in liquid Ga is a mixture of metallic and covalent types [44–46], and the covalent bonding between Ga atoms would lead to the formation of Ga clusters [44]. The structures of individual Ga clusters and their evolution have been extensively studied. Clusters consisting of different numbers of Ga atoms are shown to

possess different melting points, and most of which are higher than that of α-Ga crystal [10–16]. For instance, the clusters with 30–80 Ga atoms were experimentally observed to melt between 400 and 800 K [10,12] and the smaller clusters with 7–17 Ga atoms are reported to show much higher melting points or even no signature of melting up to 2440 K [15,47]. It should be noted that the evolution of the Ga clusters is associated with the variation of covalent bonds between Ga atoms [16,48], which would lead to the change of K_{CP}^{p} [49–51], and further contribute to K_{other}/K_d. Based on our results, a possible scenario for the structure evolution in liquid Ga is that, in the bulk liquid Ga, the Ga atoms connect to some of the nearest neighbors by covalent bonds to form different Ga clusters, and according to the relative size the clusters can be roughly classified into two categories, the "large clusters" consisting of the clusters possessing higher melting points than that of α-Ga and the "small clusters" consisting of the clusters possessing much higher melting points. Because of the fast exchange effect in liquid Ga, different structures are averaged in the NMR probe timescale, leading to a single peak in the spectra of both isotopes of Ga. At T below 1000 K, liquid Ga mainly consists of the large clusters; as the covalent bond breaking when the large clusters transform to smaller clusters at different temperatures, the variation of the covalent bonds leading to K_{other}/K_d increase. At T above 1000 K, liquid Ga mainly consists of less changed smaller clusters, thus K_{other}/K_d remains constant.

This clusters scenario is further supported by the W_Q analysis. Normally, W_Q contains temporal information on atomic jumps and diffusion, and is a reflection of the kinetic evolution in metallic liquids [37–39]. According to the ionic-diffusion model, W_Q can be expressed as [32,37,52]

$$W_Q \propto {}^{\rho}/_{D}, \tag{13}$$

where ρ is the density and D is the diffusion coefficient. Alternatively, the molecular-rotation model [53], which supposes that liquid Ga consists of Ga_2 dimers rather than single Ga ions, had also been proposed to describe the kinetics of Ga liquid, and W_Q can be expressed as [25]

$$W_Q \propto {}^{\eta V}/_{T}, \tag{14}$$

where η is the viscosity and V is a representative volume of the molecule. Figure 5 plots the normalized theoretical and experimental values of W_Q. The prediction of the ionic-diffusion model is estimated with the value of ρ from the work of Basin and Solov'ev [54] and D is estimated from the work of Xiong *et al.* [19]. The prediction of molecular-rotation model is estimated based on the work of Kerlin and Clark [32]. All curves are normalized to unity at 430 K. The deviation of the experimentally measured W_Q from the prediction of the ionic-diffusion model and molecular-rotation model implies that more complex clusters should exist in liquid Ga. At T above 1000 K, W_Q varies much slower than that at T below 1000 K, and is still deviating from theoretical prediction. Such results further indicate that clusters are less changed and can persist at T above 1000 K.

It is worth noting that a continuous variation of $K(\alpha)_{obs}$ is revealed during the whole tested temperature range, and no hysteresis is observed between the heating and cooling

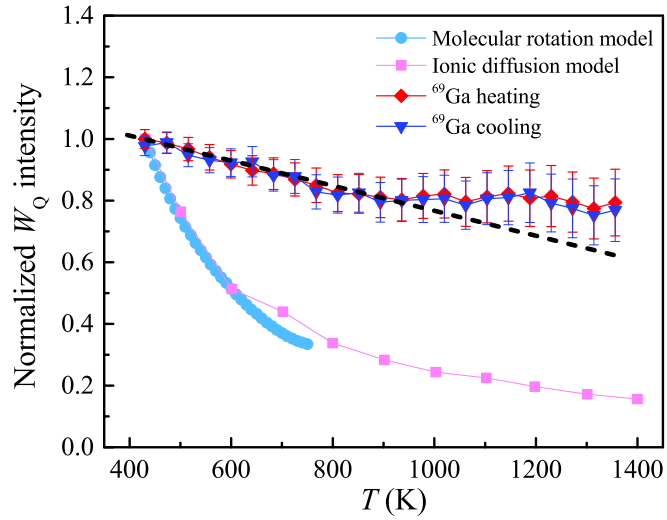

FIG. 5. Normalized values of predicted and experimental W_Q. Red rhombi and blue triangles represent the ^{69}Ga W_Q from our measurement. The dashed line is a guide for the eye.

curve of all the NMR observables, which suggests that the phenomenon we observed at around 1000 K in pure Ga melt is a structural crossover. Based on our cluster scenario, the crossover is caused by the structural evolution of liquid Ga from mainly consisting of large clusters below 1000 K to mainly consisting of small less changed clusters above 1000 K. In the two-species model description [55–57], the molar Gibbs free-energy change of covalent bonds breaking when the large clusters evolve to small clusters at constant pressure is given by [57]

$$\Delta G = X_B(\Delta H - T\Delta S) + X_B RT \ln X_B + (1 - X_B)RT \ln(1 - X_B) + W X_B(1 - X_B), \tag{15}$$

where X_B is the fraction of the total bonds which are broken at any temperature T,ΔH and ΔS are the enthalpy and entropy change per mole of broken bonds,R is the ideal gas constant, and W is the cooperativity which here means the bonds broken by the rise of temperature interacting in a way as to make the next bond broken energetically cheaper. The value of W can determine the transformation to be a crossover or a liquid-liquid transition, which was suggested to relate to the constraint of covalent bonds [57,58]. In the semiconductor element Si and Ge liquids, which may possess higher bond density per particle than Ga liquid, the overconstraint was predicted to induce a liquid-liquid transition [58–62]. The structural crossover we observed at around 1000 K may be caused by weak cooperativity resulting from the low constraint of covalent bonds in Ga liquid.

Moreover, according to the LLCP hypothesis [20–22], the critical fluctuations of LLCP are believed to be the origin of different liquid anomalies. Theoretical calculation of liquid Ga predicted that the structure anomaly and the diffusivity anomaly induced by the LLCP may appear at 450 and 730 K, respectively, at ambient pressure [24]. In our study of Ga melt, no anomalies are observed at the predicted temperatures at ambient pressure. Nonetheless, because of the existence of the

complex covalently bonded clusters, liquid Ga may not be an ideal system for verifying the LLCP hypothesis.

IV. SUMMARY

In summary, we investigated pure Ga melt in the temperature range of 307–1356 K by high-temperature ^{69}Ga and ^{71}Ga NMR. Knight shift (K_s) and spin-lattice relaxation time (T_1) were measured during consecutive heating and cooling experiments. Below and above 1000 K different T dependences are observed in the curves of all NMR observables. Further analyses suggest that more complex clusters exist in bulk liquid Ga and the changes of the NMR observables may result from the temperature-induced structural evolution of the covalently bonded Ga clusters. $K(\alpha)_{obs}$ characterizing the electronic structure varies continuously during the whole tested temperature region and no hysteresis is observed, suggesting that the structure change at around 1000 K represents a crossover which may result from the weak cooperativity induced by the low constraint of the covalent bonds. This paper furthers our understanding of the liquid structure of Ga and indicates that the complex covalent-bonding clusters can have a great impact on the structure and kinetic properties in the metallic melts, and such impact can even extend to temperatures high above the melting point. At lower temperature, such impact could become more prominent. It could be crucial for the kinetic change of supercooled liquid, and play an important role in the formation of metallic glass. In addition, the structure and diffusivity anomalies which may originate from the critical fluctuation when approaching LLCP are not observed as predicted at ambient pressure.

ACKNOWLEDGMENT

This work was supported by the National Basic Research Program of China under Grant No. 2015CB856801.

[1] N. Kazem, T. Hellebrekers, and C. Majidi, Adv. Mater. **29**, 1605985 (2017).
[2] J. W. Boley, E. L. White, G. T.-C. Chiu, and R. K. Kramer, Adv. Funct. Mater. **24**, 3501 (2014).
[3] M. A. H. Khondoker and D. Sameoto, Smart Mater. Struct. **25**, 093001 (2016).
[4] J. Zhang, Y. Yao, L. Sheng, and J. Liu, Adv. Mater. **27**, 2648 (2015).
[5] X. G. Gong, G. L. Chiarotti, M. Parrinello, and E. Tosatti, Phys. Rev. B **43**, 14277(R) (1991).
[6] E. Voloshina, K. Rosciszewski, and B. Paulus, Phys. Rev. B **79**, 045113 (2009).
[7] S.-F. Tsay and S. Wang, Phys. Rev. B **50**, 108 (1994).
[8] L.-Y. Chen, P.-H. Tang, and T.-M. Wu, J. Chem. Phys. **145**, 024506 (2016).
[9] K. H. Tsai, T.-M. Wu, and S.-F. Tsay, J. Chem. Phys. **132**, 034502 (2010).
[10] K. L. Pyfer, J. O. Kafader, A. Yalamanchali, and M. F. Jarrold, J. Phys. Chem. A **118**, 4900 (2014).
[11] G. A. Breaux, R. C. Benirschke, T. Sugai, B. S. Kinnear, and M. F. Jarrold, Phys. Rev. Lett. **91**, 215508 (2003).
[12] G. A. Breaux, D. A. Hillman, C. M. Neal, R. C. Benirschke, and M. F. Jarrold, J. Am. Chem. Soc. **126**, 8628 (2004).
[13] K. G. Steenbergen, D. Schebarchov, and N. Gaston, J. Chem. Phys. **137**, 144307 (2012).
[14] A. Susan, A. Kibey, V. Kaware, and K. Joshi, J. Chem. Phys. **138**, 014303 (2013).
[15] S. Chacko, K. Joshi, D. G. Kanhere, and S. A. Blundell, Phys. Rev. Lett. **92**, 135506 (2004).
[16] S. Krishnamurty, S. Chacko, D. G. Kanhere, G. A. Breaux, C. M. Neal, and M. F. Jarrold, Phys. Rev. B **73**, 045406 (2006).
[17] O. F. Yagafarov, Y. Katayama, V. V. Brazhkin, A. G. Lyapin, and H. Saitoh, High Pressure Res. **33**, 191 (2013).
[18] R. Li, L. Li, T. Yu, L. Wang, J. Chen, Y. Wang, Z. Cai, J. Chen, M. L. Rivers, and H. Liu, Appl. Phys. Lett. **105**, 041906 (2014).
[19] L. Xiong, X. Wang, Q. Yu, H. Zhang, F. Zhang, Y. Sun, Q. Cao, H. Xie, T. Xiao, and D. Zhang, Acta Mater. **128**, 304 (2017).
[20] P. H. Poole, F. Sciortino, U. Essmann, and H. E. Stanley, Nature (London) **360**, 324 (1992).
[21] O. Mishima and H. E. Stanley, Nature (London) **392**, 164 (1998).
[22] Y. Li, J. Li, and F. Wang, Proc. Natl. Acad. Sci. USA **110**, 12209 (2013).
[23] D. A. Carvajal Jara, M. Fontana Michelon, A. Antonelli, and M. de Koning, J. Chem. Phys. **130**, 221101 (2009).
[24] R. Li, G. Sun, and L. Xu, J. Chem. Phys. **145**, 054506 (2016).
[25] A. Abragam, *The Principles of Nuclear Magnetism* (Oxford University, New York,1961).
[26] C. P. Slichter, *Principles of Magnetic Resonance* (Springer, New York, 1996.
[27] J. Titman, Phys. Rep. **33**, 1 (1977).
[28] D. A. Cornell, Phys. Rev. **153**, 208 (1967).
[29] D. Hechtfischer, R. Karcher, and K. Luders, J. Phys. F **3**, 2021 (1973).
[30] K. Suzuki and O. Uemura, J. Phys. Chem. Solids **32**, 1801 (1971).
[31] G. Cartledge, R. Havill, and J. Titman, J. Phys. F **3**, 213 (1973).
[32] A. Kerlin and W. Clark, Phys. Rev. B **12**, 3533 (1975).
[33] E. V. Charnaya, C. Tien, W. Wang, M. K. Lee, D. Michel, D. Yaskov, S. Y. Sun, and Y. A. Kumzerov, Phys. Rev. B **72**, 035406 (2005).
[34] L. Li and Y. Wu, J. Chem. Phys. **128**, 052307 (2008).
[35] F. Faupel, W. Frank, M.-P. Macht, H. Mehrer, V. Naundorf, K. Rätzke, H. R. Schober, S. K. Sharma, and H. Teichler, Rev. Mod. Phys. **75**, 237 (2003).
[36] W. W. Warren, Jr. and W. G. Clark, Phys. Rev. **177**, 600 (1969).
[37] C. Sholl, Proc. Phys. Soc. **91**, 130 (1967).
[38] C. Sholl, J. Phys. F **4**, 1556 (1974).
[39] W. Xu, M. T. Sandor, Y. Yu, H.-B. Ke, H.-P. Zhang, M.-Z. Li, W.-H. Wang, L. Liu, and Y. Wu, Nat. Comm. **6**, 7696 (2015).
[40] C. H. Townes, C. Herring, and W. D. Knight, Phys. Rev. **77**, 852 (1950).
[41] A. Narath, in *Hyperfine Interactions*, edited A. J. Freeman and R. B. Frankel (Academic, New York, 1967).
[42] A. Narath and H. Weaver, Phys. Rev. **175**, 373 (1968).

[43] R. W. Shaw, Jr. and W. W. Warren, Jr., Phys. Rev. B **3**, 1562 (1971).
[44] F. J. Bermejo, I. Bustinduy, S. J. Levett, J. W. Taylor, R. Fernández-Perea, and C. Cabrillo, Phys. Rev. B **72**, 104103 (2005).
[45] S. Hosokawa, W. C. Pilgrim, H. Sinn, and E. E. Alp, J. Phys.: Condens. Matter **20**, 114107 (2008).
[46] P. Ghigna, G. Spinolo, G. B. Parravicini, A. Stella, A. Migliori, and R. Kofman, J. Am. Chem. Soc. **129**, 8026 (2007).
[47] K. G. Steenbergen and N. Gaston, Physical Chem. Chem. Phys. **15**, 15325 (2013).
[48] S. Krishnamurty, K. Joshi, S. Zorriasatein, and D. G. Kanhere, J. Chem. Phys. **127**, 054308 (2007).
[49] V. Kaware and K. Joshi, J. Chem. Phys. **141**, 054308 (2014).
[50] W.-M. Shyu, T. Das, and G. Gaspari, Phys. Rev. **152**, 270 (1966).
[51] R. Kasowski and L. Falicov, Phys. Rev. Lett. **22**, 1001 (1969).
[52] W. Schirmacher, Ber. Bunsenges. Phys. Chem. **80**, 736 (1976).
[53] T. E. Faber, Solid State Commun. **1**, 41 (1963).
[54] A. Basin and A. Solov'ev, J. Appl. Mech. Tech. Phys. **8**, 57 (1967).
[55] E. Rapoport, J. Chem. Phys. **46**, 2891 (1967).
[56] C. T. Moynihan, MRS Online Proc. Libr. **455**, 411 (1996).
[57] C. A. Angell and C. T. Moynihan, Metall. Mater. Trans. B **31**, 587 (2000).
[58] C. A. Angell, B. E. Richards, and V. Velikov, J. Phys.: Condens. Matter **11**, A75 (1999).
[59] C. A. Angell, S. Borick, and M. Grabow, J. Non-Cryst. Solids **205–207**, 463 (1996).
[60] M. Togaya, Phys. Rev. Lett. **79**, 2474 (1997).
[61] P. F. McMillan, M. Wilson, D. Daisenberger, and D. Machon, Nat. Mater. **4**, 680 (2005).
[62] J. T. Okada, P. H.-L. Sit, Y. Watanabe, Y. J. Wang, B. Barbiellini, T. Ishikawa, M. Itou, Y. Sakurai, A. Bansil, R. Ishikawa *et al.*, Phys. Rev. Lett. **108**, 067402 (2012).